

Green synthesis of fluorescent carbon nanoparticles from Lychee (*Litchi chinensis*) plant

Vidhi Chaudhary[†] and Anil Kumar Bhowmick[‡]

Sophisticated Advanced Instrumentation Facility, Indian Institute of Technology Patna,
Patliputra Colony, Patna- 800013, Bihar, India

(Received 19 August 2014 • accepted 20 December 2014)

Abstract—Fluorescent carbon nanoparticles (CNPs) were prepared from waste lychee peel by hydrothermal process using green chemistry. These CNPs were characterized by UV-vis absorption, fluorescence spectroscopy, Fourier transform infrared spectroscopy (FTIR) and X-ray diffraction. Their morphology was analyzed by field emission scanning electron microscopy. Spherical carbon nanoparticles with a particle size ranging from 40-70 nm were observed. FTIR data indicated that these CNPs were functionalized with hydroxyl and carboxylic or carbonyl group. The maximum fluorescence intensity for these CNPs was observed on the excitation wavelength at 365 nm with emission maxima centered at 450 nm. These particles exhibited excitation wavelength dependent fluorescence emission spectra. CNPs were found to be highly fluorescent and exhibited high water solubility. The band gap was estimated to be 3.8 eV. Therefore, as prepared CNPs would be useful in bioimaging, biolabeling and in the other applications of nanobiotechnology.

Keywords: Green Synthesis, Carbon Nanoparticles, Fluorescence, Nanobiotechnology, Lychee

INTRODUCTION

Synthesis of carbon based nanomaterials and related hybrid/composite materials is a hot topic of current research due to their potential applications in science and technology. Carbon nanomaterials are found in various forms such as carbon nanotube, carbon nanoribbon, carbon nanofiber, fullerene, graphene and carbon dots (CDs)/carbon nanoparticles (CNPs) [1-13]. Carbon nanoparticles are interesting for research due to their fluorescence property as compared to semiconductor nanoparticles and fluorescent dye probes. Semiconductor nanoparticles have been extensively used for biolabeling and bioimaging in bio-applications because of their fluorescence property [14]. But these inorganic semiconductor nanoparticles are highly toxic and environmentally hazardous. So their use for bio-application and *in vivo* application in human is limited. Due to their high water solubility, low toxicity and better biocompatibility, fluorescent CNPs can be better alternative for the *in vivo* biolabeling and in other bio-medical applications. So, CNPs have potential application in nanobiotechnology, catalysis and optoelectronic devices [15-19]. CDs passivated with poly (propionylethylenimine-co-ethylenimine) were first reported by Sun et al. for two-photon, luminescence microscopy imaging of human breast cancer cells [20]. Photoreduction of Ag^+ to Ag by photoirradiating CDs in an aqueous solution of AgNO_3 was confirmed earlier, which represents the electron-donor capabilities of photoexcited carbon dots [21]. Some researchers have also used the CNPs as fluorescent probe

for the detection of Hg^{2+} and hypochlorite [22,23].

In last decade, a large number of synthetic methods, such as ultrasonic, microwave, acidic oxidation, electrochemical oxidation, thermal oxidation of suitable molecular precursors and laser ablation have been used for the preparation of CNPs [24-30]. Conversely, these methodologies for the preparation of CNPs have some drawbacks like high temperature, time consuming, high cost and severe reaction conditions. Green synthesis for the nanomaterials has some advantages: environmentally friendly, low cost and mild reaction condition. Also, generalizing nanoparticles from waste material has gained importance in recent years. In this work, we have reported the green synthesis of CNPs from lychee peel (waste material), which is environmentally friendly and derived from a low cost method.

Lychee (*Litchi chinensis*) is an evergreen, subtropical fruit tree, native to south China. India has also the good production of lychee, especially in Muzaffarpur city at Bihar. To the best of our knowledge, there is no article reported on the green synthesis of CNPs from waste lychee plant till now.

In this work, we have prepared CNPs using lychee peel, by a hydrothermal process. These CNPs have been characterized by FTIR, XRD, FESEM, UV-visible absorption and fluorescence spectroscopy. As prepared CNPs may find their suitable applications in nanobiotechnology, catalysis and optoelectronic devices.

EXPERIMENTAL SECTION

1. Materials

Lychee fruits were purchased from local fruit shop, Patna (Bihar). Double distilled water was used in the whole experiment. Lychee fruits were washed properly with double distilled water before experiment.

2. Synthesis of CNPs

First, the lychee peels were collected from the lychee fruit, dried

[†]To whom correspondence should be addressed.

E-mail: vc@iitp.ac.in

[‡]Current address: Rubber Technology Center, Indian Institute of Technology, Kharagpur 721302, India

Copyright by The Korean Institute of Chemical Engineers.

and crushed with the help of mortar pistil. In the process, 1 g of crushed lychee peel was mixed with double distilled water. The mixture was poured into a 25 ml Teflon-lined autoclave followed by heating at 180 °C for three hours. CNPs were collected by removing the large material through centrifugation at 15,000 rpm for 15 min. The final product was kept under vacuum in a vacuum oven for three days and the dried product was obtained. For further characterization of CNPs, 0.3 mg/ml of CNPs was dispersed in double distilled water. The solubility of these CNPs was checked in ethanol and acetone. After sonication, they were found to be soluble in respective solvents.

3. Characterization

UV-vis absorption spectrum of as prepared CNPs was recorded from Shimadzu UV-vis spectrophotometer (Model UV-2550) by using a 1 cm quartz cell. The fluorescence emission measurements were performed on a Fluoromax-4P spectrofluorometer (Horiba Jobin Yvon). The morphology of the CNPs was studied with the help of field emission scanning electron microscope (FESEM) (Hitachi, S-4800) by applying accelerating voltage of 5-10 kV. Small amount of the sample, dispersed in acetone, was put on a conducting car-

bon tape and coated with platinum by using Hitachi E-1010 Ion sputter system. X-ray diffraction (XRD) data were recorded in the 2θ range from 10 to 80° using a Rigaku TT RAX 3 with Cu K α radiation (30 kV, 20 mA, $\lambda=0.154$ nm). FTIR spectrum of the CNPs was obtained from a Perkin Elmer FTIR spectrophotometer (Model-spectrum 400), within a range of 400-4,000 cm^{-1} using a resolution of 16 cm^{-1} .

RESULTS AND DISCUSSION

UV-visible absorption spectrum of the CNPs extracted from lychee peel is shown in Fig. 1(a), which exhibits a strong peak at 281 nm. The peak at 281 nm might be ascribed to the $n-\pi^*$ transition of C=O band. This absorption spectrum of as prepared CNPs displayed similar features to those of CNPs synthesized from pomelo peel [22], suggesting the presence of CNPs in the product. Production of CNPs from ascorbic acid exhibits analogous peak in their UV-vis absorption spectrum [31]. The band gap of the CNPs was estimated to be 3.8 eV. It was determined by the extrapolation of the linear portion of the curve to X-axis as shown in Fig. 1(b). This value of the band gap of the CNPs is slightly higher than that of the conventional semiconductor gallium nitride (band gap=3.4 eV) [32], suggesting the semiconducting nature of the as prepared CNPs.

Fluorescence emission spectrum of CNPs is represented in Fig. 2(a). It was observed that the maximum emission intensity was obtained with the excitation wavelength of 365 nm, in which emission maxima peak was centered at 450 nm. The photograph of the CNPs dispersed in water shows a blue color (Fig. 2(a) - Inset) under UV light excitation that also exhibits blue fluorescence of the as prepared CNPs. These CNPs show excitation dependent emission spectra (Fig. 2(b)). The emission intensity of the CNPs decreased with the increase in excitation wavelength from 365 to 480 nm, along with red shift in the emission maxima (Fig. 2(b)-2(c)), exhibiting the excitation tunable emission property. It was earlier reported that CNPs show photoluminescence property due to the presence of different surface trap sites [33]. This excitation dependent property could be attributed to the distribution of the different particle size of CNPs. The quantum yield of CNPs was calculated by using the following relation:

$$\Phi = \Phi_R \times \frac{I}{I_R} \times \frac{A_R}{A} \times \frac{n^2}{n_R^2} \quad (1)$$

where Φ is the quantum yield, A is the absorbance, I is the integrated emission intensity and n is the refractive index. The subscript R refers to the reference sample. The fluorescence quantum yield of CNPs was calculated to be 21% (Table 1) at an excitation wavelength 365 nm by using quinine sulfate (quantum yield=54%) as a reference standard sample [12]. The value of quantum yield of CNPs was comparatively higher than that of CNPs obtained by other methods [11,22]. FESEM image of the as synthesized CNPs is shown in Fig. 3(a). This image shows that the particle size of the CNPs ranges from 40 to 70 nm in the aggregates. An EDX analysis of the sample reveals (Fig. 3(b)) the presence of carbonaceous phase with little amount of oxygen. Maximum intensity of the carbon peak in EDX spectrum shows the formation of carbon nanoparticles. The presence of oxygen in very small amount is observed due to the

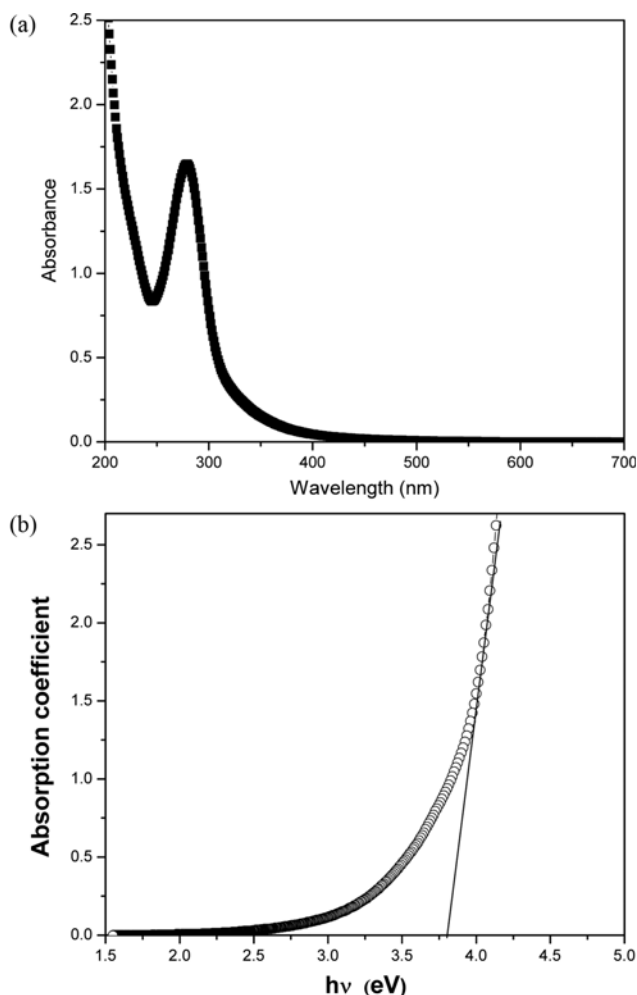


Fig. 1. (a) UV-visible absorption spectrum of the CNPs. (b) UV-visible absorption spectrum replotted to estimate the band gap of CNPs.

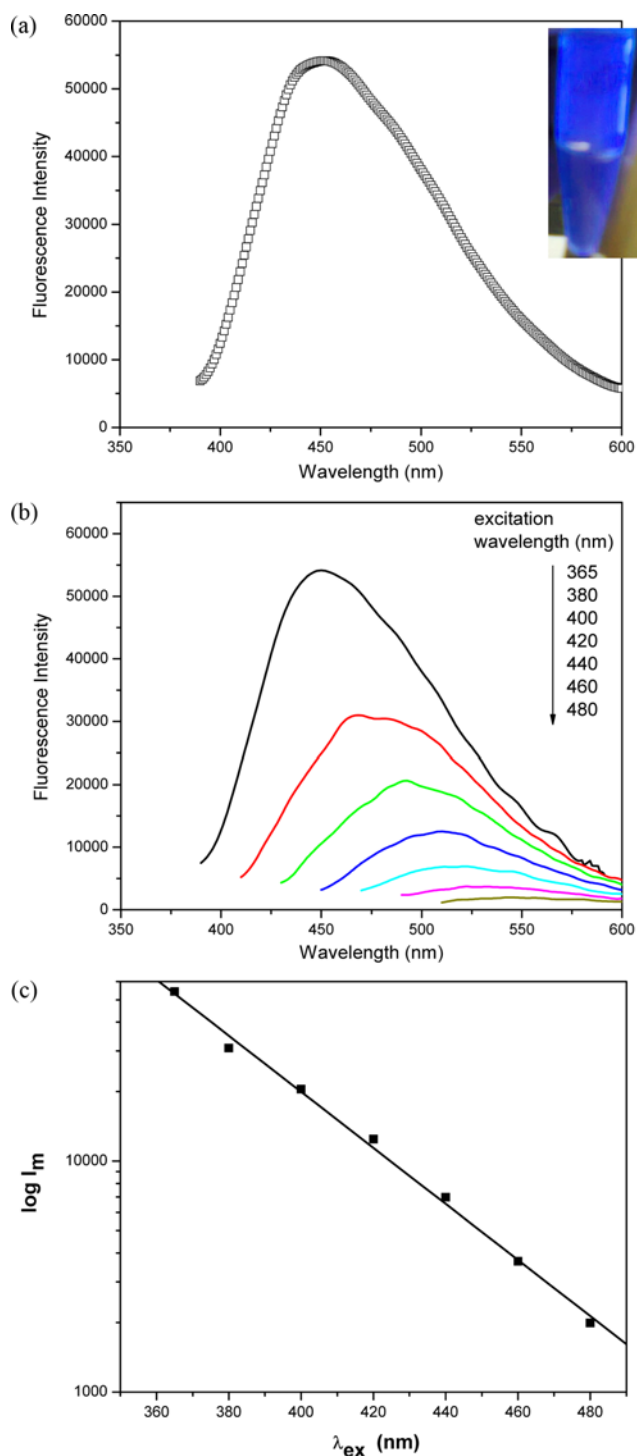
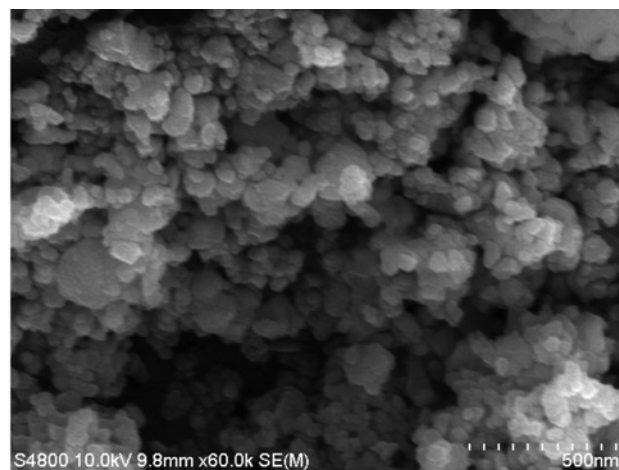


Fig. 2. (a) Emission spectrum of the CNPs excited at 365 nm. Inset exhibits the photograph of aqueous dispersion of CNPs under UV light ($\lambda_{ex}=365$ nm). (b) Emission spectra of the CNPs at excitation wavelengths increasing from 365 nm to 480 nm. (c) Effect of the excitation wavelength (λ_{ex}) on the fluorescence emission intensity (I_m) of CNPs.

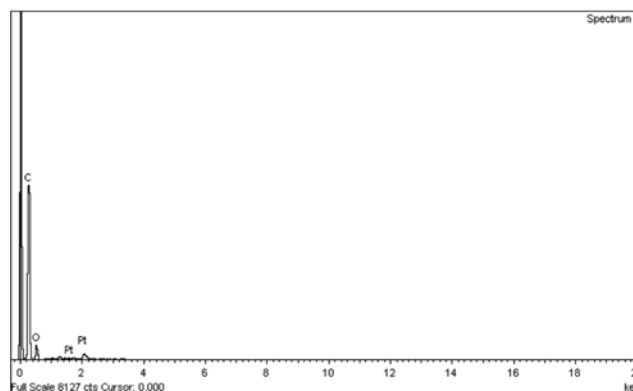
oxidation of carbon during carbonization process. In EDX spectrum, the platinum (Pt) peak is coming due to coating of the Pt during the sample preparation.

Table 1. Quantum yield of CNPs

Sample	Integrated emission intensity (I)	Absorbance (A)	Refractive index of solvent (η)	Quantum yield (Φ)
Quinine sulfate	48560	0.055	1.33	0.54
CNPs sample	54000	0.157	1.33	0.21



(a)



(b)

Fig. 3. (a) FESEM image of the CNPs. (b) EDX spectrum of the CNPs.

FTIR spectrum of these CNPs is shown in Fig. 4. The peaks at $3,390$ and $1,050$ cm^{-1} correspond to the -OH stretching vibration mode and the peak at $1,256$ cm^{-1} is attributed to the C-OH stretching mode. The sharp peaks at $1,610$ and $1,404$ cm^{-1} are attributed to the asymmetric and symmetric stretching vibration of carboxylate anions, respectively [34]. A peak at $2,929$ cm^{-1} is also observed, which is attributed to the C-H stretching mode. The FTIR results show that the as-prepared CNPs were functionalized with hydroxyl and carboxylic or carbonyl groups. The carbohydrates present in the lychee peel are responsible for these polar groups. The formation of carbon nanoparticles from carbohydrates is a complex process. It was also not possible to take out samples from time to time and analyze the complex mixture. However, one possible mechanism is proposed for the production of these CNPs as shown in the Scheme 1, which is based on the carbonization of carbohydrates

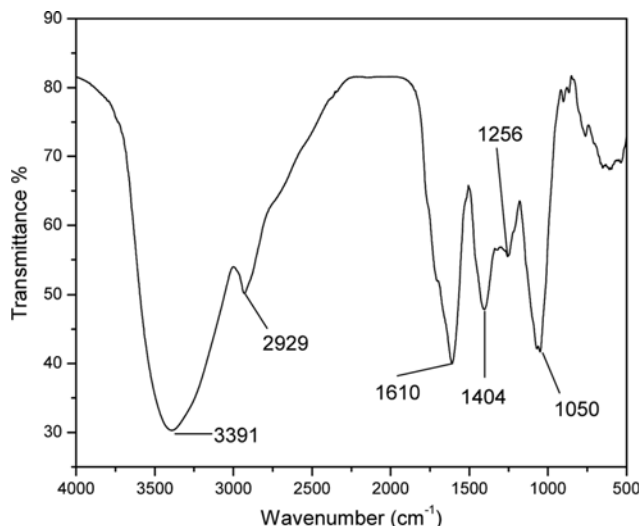
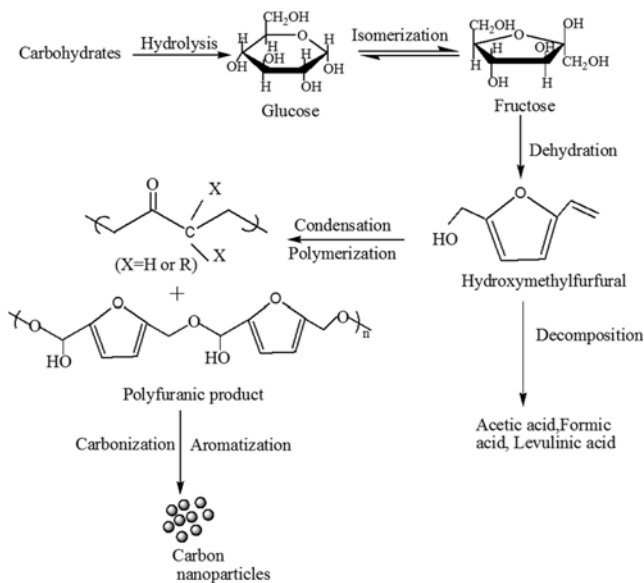


Fig. 4. FT-IR spectrum of the CNPs.



Scheme 1. Possible reaction mechanism for the formation of CNPs.

[35]. This mechanism is followed by hydrolysis, dehydration and decomposition of different carbohydrate in lychee and the formation of some compounds like hydroxyl methyl furfural, furfural aldehyde, ketones, formic acid, acetic acid, and levulinic acid. The hydronium ions formed from these acids act as a catalyst in subsequent reaction process. The condensation and polymerization of these products yield the formation of different polymeric products. Finally, the CNPs are produced from the nuclear burst of these concentrated aromatic products at a supersaturation point. The proposed mechanism is also supported by the literature on carbonization of carbohydrates [35,36].

Fig. 5 represents the XRD pattern of CNPs. XRD pattern shows a broad peak located at 20° with an inter layer spacing of 0.44 nm, which is larger than that of the graphite (0.34 nm). These results indicate that the peak is not sharp due to the introduction of oxy-

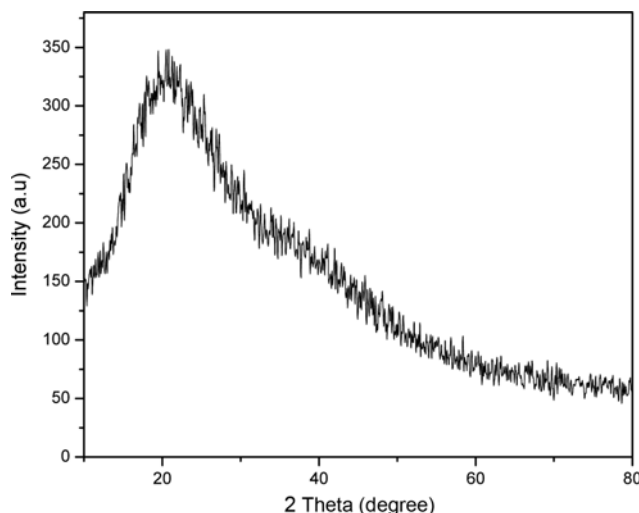


Fig. 5. XRD of the CNPs.

gen-containing groups [37]. The XRD data corroborate the FTIR spectrum of CNPs. These CNPs were found stable for several months without any precipitation due to the electrostatic repulsion between the particles.

CONCLUSIONS

Fluorescent CNPs were prepared by a simple green chemistry approach based on the hydrothermal process of waste lychee peel. The scanning electron micrograph of CNPs revealed the formation of spherical nanoparticles of 40 to 70 nm. FTIR study of CNPs confirmed their functionalization with hydroxyl and carboxylic or carbonyl groups due to the presence of carbohydrate in the lychee peel. Under UV light excitation, CNPs exhibited blue fluorescence. The estimated band gap (3.8 eV) of CNPs suggested their semi-conducting behavior. These CNPs showed high fluorescence property and high water solubility. Such fluorescent CNPs could be useful in bioimaging and biolabeling application in nanobiotechnology.

ACKNOWLEDGEMENT

The financial support of IIT, Patna for performing this study is gratefully acknowledged. VC is thankful to the Director, IIT Patna, for providing the laboratory and instrumentation facilities.

REFERENCES

1. J. M. O'Connell, S. M. Bacilo, C. B. Huffman, V. C. Moore, M. S. Strano, E. H. Haroz, K. L. Rialon, P. J. Boul, W. H. Noon, C. Kittrell, J. Ma, R. H. Hauge, R. B. Weisman and R. E. Smalley, *Science*, **297**, 593 (2002).
2. N. Roy, R. Sengupta and A. K. Bhowmick, *Progress Polym. Sci.*, **37**, 781 (2012).
3. M. Kotal, A. K. Thakur and A. K. Bhowmick, *ACS Appl. Mater. Interfaces*, **5**, 8374 (2013).
4. H. T. Li, Z. H. Kang, Y. Liu and S. T. Lee, *J. Mater. Chem.*, **22**, 24230

- (2012).
5. S. N. Baker and G. A. Baker, *Angew. Chem. Int. Ed.*, **49**, 6726 (2010).
 6. J. Lu, J.-X. Yang, J. Wang, A. Lim, S. Wang and K. P. Loh, *ACS Nano*, **3**, 2367 (2009).
 7. S. Iijima, *Nature*, **354**, 56 (1991).
 8. N. Roy and A. K. Bhowmick, *J. Appl. Polym. Sci.*, **123**, 3675 (2012).
 9. H. Kohno, T. Komine, T. Hasegawa, H. Niioka and S. Ichikawa, *Nanoscale*, **5**, 570 (2013).
 10. M.-Q. Yang, N. Zhang and Y.-J. Xu, *ACS Appl. Mater. Interfaces*, **5**, 1156 (2013).
 11. H. Liu, T. Ye and C. Mao, *Angew. Chem. Int. Ed.*, **46**, 6473 (2007).
 12. B. Chen, F. Li, S. Li, W. Wang, H. Guo, T. Guo, X. Zhang, Y. Chen, T. Huang, X. Hong, S. You, Y. Lin, K. Zeng and S. Chen, *Nanoscale*, **5**, 1967 (2013).
 13. S. Sahu, B. Behera, T. K. Maiti and S. Mohapatra, *Chem. Commun.*, **48**, 8835 (2012).
 14. X. Michalet, F. F. Pinaud, L. A. Bentolila, J. M. Tsay, S. Doose, J. J. Li, G. Sundaresan, A. M. Wu, S. S. Gambhir and S. Weiss, *Science*, **307**, 538 (2005).
 15. J. Shen, Y. Zhu, X. Yang and C. Li, *Chem. Commun.*, **48**, 3686 (2012).
 16. W. Shi, Q. Wang, Y. Long, Z. Cheng, S. Chen, H. Zheng and Y. Huang, *Chem. Commun.*, **47**, 6695 (2011).
 17. S. C. Ray, A. Saha, N. R. Jana and R. Sarkar, *J. Phys. Chem. C*, **113**, 18546 (2009).
 18. R. Liu, D. Wu, S. Liu, K. Koynov, W. Knoll and Q. Li, *Angew. Chem. Int. Ed.*, **48**, 4598 (2009).
 19. H. Li, X. He, Z. Kang, H. Huang, Y. Liu, J. Liu, S. Lian, C. H. A. Tsang, X. Yang and S.-T. Lee, *Angew. Chem. Int. Ed.*, **49**, 4430 (2010).
 20. Y.-P. Sun, B. Zhou, Y. Lin, W. Wang, K. A. S. Fernando, P. Pathak, M. J. Meziani, B. A. Harruff, X. Wang, H. Wang, P. G. Luo, H. Yang, M. E. Kose, B. Chen, L. M. Veca and S.-Y. Xie, *J. Am. Chem. Soc.*, **128**, 7756 (2006).
 21. X. Wang, L. Cao, F. Lu, M. J. Meziani, H. Li, G. Qi, B. Zhou, B. A. Harruff, F. Kermarrec and Y.-P. Sun, *Chem. Commun.*, **25**, 3774 (2009).
 22. W. Lu, X. Qin, S. Liu, G. Chang, Y. Zhang, Y. Luo, A. M. Asiri, A. O. A. Youbi and X. Sun, *Anal. Chem.*, **84**, 5351 (2012).
 23. B. Yin, J. Deng, X. Peng, Q. Long, J. Zhao, Q. Lu, Q. Chen, H. Li, H. Tang, Y. Zhang and S. Yao, *Analyst*, **138**, 6551 (2013).
 24. H. Li, X. He, Y. Liu, H. Huang, S. Lian, S.-T. Lee and Z. Kang, *Carbon*, **49**, 605 (2011).
 25. X. Wang, K. Qu, B. Xu, J. Rena and X. Qu, *J. Mater. Chem.*, **21**, 2445 (2011).
 26. L. Tian, D. Ghosh, W. Chen, S. Pradhan, X. J. Chang and S. W. Chen, *Chem. Mater.*, **21**, 2803 (2009).
 27. J. Zhou, C. Booker, R. Li, X. Zhou, T.-K. Sham, X. Sun and Z. Ding, *J. Am. Chem. Soc.*, **129**, 744 (2007).
 28. A. B. Bourlinos, A. Stassinopoulos, D. Anglos, R. Zboril, M. Karakassides and E. P. Giannelis, *Small*, **4**, 455 (2008).
 29. S. L. Hu, K. Y. Niu, J. Sun, J. Yang, N. Q. Zhao and X. W. Du, *J. Mater. Chem.*, **19**, 484 (2009).
 30. X. Qin, W. Lu, A. M. Asiri, A. O. Al-Youbi and X. Sun, *Sensors and Actuators B: Chem.*, **184**, 156 (2013).
 31. X. Jia, J. Li and E. Wang, *Nanoscale*, **4**, 5572 (2012).
 32. B. G. Streetman and S. Banerjee, *Solid State Electronic Devices*, Prentice Hall, New Jersey (2000).
 33. A. Salinas-Castillo, M. Ariza-Avidad, C. Pritz, M. Camprubi-Robles, B. Fernandez, M. J. Ruedas-Rama, A. Megia-Fernandez, A. Lapresta-Fernandez, F. Santoyo-Gonzalez, A. Schrott-Fischer and L. F. Capitán-Vallvey, *Chem. Commun.*, **49**, 1103 (2013).
 34. M. J. Bojdys, J.-O. Muller, M. Antonietti and A. Thomas, *Chem. Eur. J.*, **14**, 8177 (2008).
 35. B. De and N. Karak, *RSC Advance*, **3**, 8286 (2013).
 36. C. Falco, N. Baccile and M.-M. Titirici, *Green Chem.*, **13**, 3273 (2011).
 37. J. Peng, W. Gao, B. K. Gupta, Z. Liu, R. Romero-Aburto, L. Ge, L. Song, L. B. Alemany, X. Zhan, G. Gao, S. A. Vithayathil, B. A. Kaiparettu, A. A. Marti, T. Hayashi, J. Zhu and P. M. Ajayan, *Nano Lett.*, **12**, 844 (2012).